RSC Advances

PAPER

View Article Online
View Journal | View Issue

Cite this: RSC Adv., 2017, 7, 12277

Combating fuel-driven aqua-pollution using "benzomagnets"

Zaki S. Seddigi,[a] Saleh A. Ahmed,*[b] Samim Sardar,[c] Naeema H. Yarkandi,[b] Mohammed Abdulaziz[a] and Samir Kumar Pal*[c]

Marine environments are frequently exposed to semi-volatile polyaromatic hydrocarbons (PAHs) from anthropogenic sources including the incomplete combustion of fossil fuels or oil spills. Benzo[*a*]pyrene (BP), one of the most dangerous PAHs, has been found to be the champion killer of marine life due to its potent mutagenicity and carcinogenicity. Herein, we developed a novel porous microsphere comprising a nanohybrid of TiO_2 nanoparticles (~20 nm diameter) and a biologically relevant dye (protoporphyrin IX) for the complete removal of BP from aqueous environments. Steady state/picosecond-resolved spectroscopy and high-resolution electron microscopy were used for the structural characterization of the functional microspheres (FMs). The FMs were found to adsorb the dispersed BP with almost cent percent efficiency for several cycles with photo/chemical recharging options. We deposited the FMs onto a stainless steel mesh to fabricate a prototype for future marine application in the real-world removal of pollution. We also designed an assessment strip using the FMs for the rapid onboard monitoring of BP contamination in any aqueous environment, which was found to detect ppm (25 micromolar) and ppt (50 picomolar) levels of BP using absorption and fluorometric assays, respectively.

Received 12th November 2016
Accepted 6th February 2017

DOI: 10.1039/c6ra26683e

rsc.li/rsc-advances

1. Introduction

Marine ecosystem is vulnerable to frequent oil spills during the global transportation of fossil fuels.[1] The contamination of seawater with polyaromatic hydrocarbons (PAHs) associated with oil spills has been well documented in the literature and has been reported to cause decades of havoc on marine and coastal ecosystems.[2] While a global assessment of the occurrence and atmosphere-ocean fluxes of PAHs is very crucial, the previously reported data have been severely questioned. The concentration of carbon deposition due to anthropogenic sources has been estimated to be 400 Tg C per year, which is around 15% of the oceanic CO_2 uptake.[3] The consequences of large oil spills have been widely reported; however, more common and frequent small spills still need to be considered.[4] In a recent report, it has been pointed out that even small spills have immediate adverse biological effects and their recurrent nature is likely to affect the marine ecosystems, functioning in a much more adverse way in contrary to common thinking.[5] Supervised oil spill experiments found that the dissolved and dispersed oil components become available to marine biota within a few hours even at depth of 8 meters below the spill.[5] To date, the remediation measures for oil spills rely on hydrocarbon-degrading microorganisms. To initiate the breakdown of certain hydrocarbons (*e.g.* PAHs), the microorganisms produce enzymes and biological surfactants that facilitate the degradation process.[6] Chemical surfactants are also routinely used as dispersants for the PAH-contaminated waters as an emergency response to marine oil spills.[7] The dispersants are proposed to expose the PAH molecules to marine microorganisms for degradation. However, the activity of the enzymes from the microorganisms towards PAHs in the presence of chemical dispersants is poorly understood and makes the bioremediation process uncertain.[8] A recent study has demonstrated that chlorophyll from algal blooms accelerates the photodegradation of benzo[*a*]pyrene (BP), which should be more applicable to wastewater treatment.[9]

In the abovementioned context, it is clear that a physical treatment strategy for the demonstration of PAH-exposed marine water due to accidental oil spillage is in utmost need and surprisingly absent in the literature. In the present study, functional microspheres (FMs) comprising TiO_2 nanoparticles and an organic dye, protoporphyrin IX (PP), which is of a biological origin, were synthesized. The FMs can be easily attached to stainless steel mesh for potential marine applications. The complete removal of BP from an aqueous environment using the FMs and their recharging *via* physical (solar) and chemical

[a]*Department of Environmental Health, Faculty of Public Health and Health Informatics, Umm Al-Qura University, 21955 Makkah, Saudi Arabia*

[b]*Chemistry Department, Faculty of Applied Sciences, Umm Al-Qura University, 21955 Makkah, Saudi Arabia. E-mail: saleh_63@hotmail.com*

[c]*Department of Chemical, Biological and Macromolecular Sciences, S. N. Bose National Centre for Basic Sciences, Block JD, Sector III, SaltLake, Kolkata 700 106, India. E-mail: skpal@bose.res.in*

(acetonitrile) methods were demonstrated. Moreover, we showed that the FMs can be used as an onboard assessment tool for the detection of BP contamination at the ppt level. The sensitivity can be further increased by optimizing the time and area of exposure of the FMs to the environment under assessment. The development and potential application of the nanomaterials may find relevance in the physical remediation of marine environments that are under an accidental exposure to dangerous PAHs, including BP, and in wastewater management (assessment and cleaning of BP).

2. Materials and methods

2.1. Reagents

Titanium isopropoxide, protoporphyrin IX, benzo[*a*]pyrene, and iron(III) chloride were purchased from Sigma-Aldrich. Ultrapure water (Millipore System, 18.2 MΩ cm), acetonitrile, dimethyl sulphoxide, and acetone (Merck) were used as solvents. Analytical grade chemicals were used without any further purification.

2.2. Synthesis of TiO_2 microspheres

The synthesis of mesoporous TiO_2 microspheres was performed using a literature procedure.[10] A mixture of titanium isopropoxide (1 mL) and anhydrous acetone (15 mL) was stirred for 15 min and the resulting solution was transferred into a Teflon lined stainless-steel autoclave. The autoclave was heated at 180 °C for 12 h. The resulting precipitate was collected, washed several times with acetone and ethanol, and then dried over a water bath at 60 °C.

2.3. Synthesis of TiO_2 microsphere-containing mesh

To prepare microspheres on a stainless steel mesh, initially, the mesh was cleaned *via* ultrasonication in acetone, water, and ethanol for 10 min each and then dried. The deposition of titanium isopropoxide (in acetone) on the mesh was carried out using a nebulizer followed by annealing at 400 °C for 4 hours, which was used as a seeding layer for the synthesis of TiO_2 microspheres. Then, the mesh was placed in a 20 mL Teflon lined stainless-steel autoclave with titanium isopropoxide as described in the earlier section and heated at 180 °C for 12 h. Then, the mesh was thoroughly washed with acetone and then with water to remove the excess unreacted reagents. The as-synthesized TiO_2 microspheres on the mesh were further annealed at 400 °C for 1 h in the air.

2.4. Sensitization of TiO_2 microspheres (MS) and TiO_2 microsphere-containing mesh with protoporphyrin IX (PP)

A 0.5 mM PP solution in DMSO was prepared under constant stirring for 15 min. TiO_2 MS was added into a 0.5 mM dye solution at room temperature and stirred for 12 hours in the dark. Then, the solution was centrifuged for a few minutes. To remove the unattached dyes, the clear supernatant solution was decanted and the residue was washed with ethanol. This process was repeated several times. The material (nanohybrid) was then dried over a water bath at 60 °C and stored in the dark until further use. For the synthesis of Fe(III)PP, we used 1 : 1 PP (0.5 mM) and metal ions (iron(III) chloride) in DMSO/water (1 : 1) and stirred the mixture for 12 h. After the metalation step, the mixture of TiO_2 MS and Fe(III)PP solution was stirred

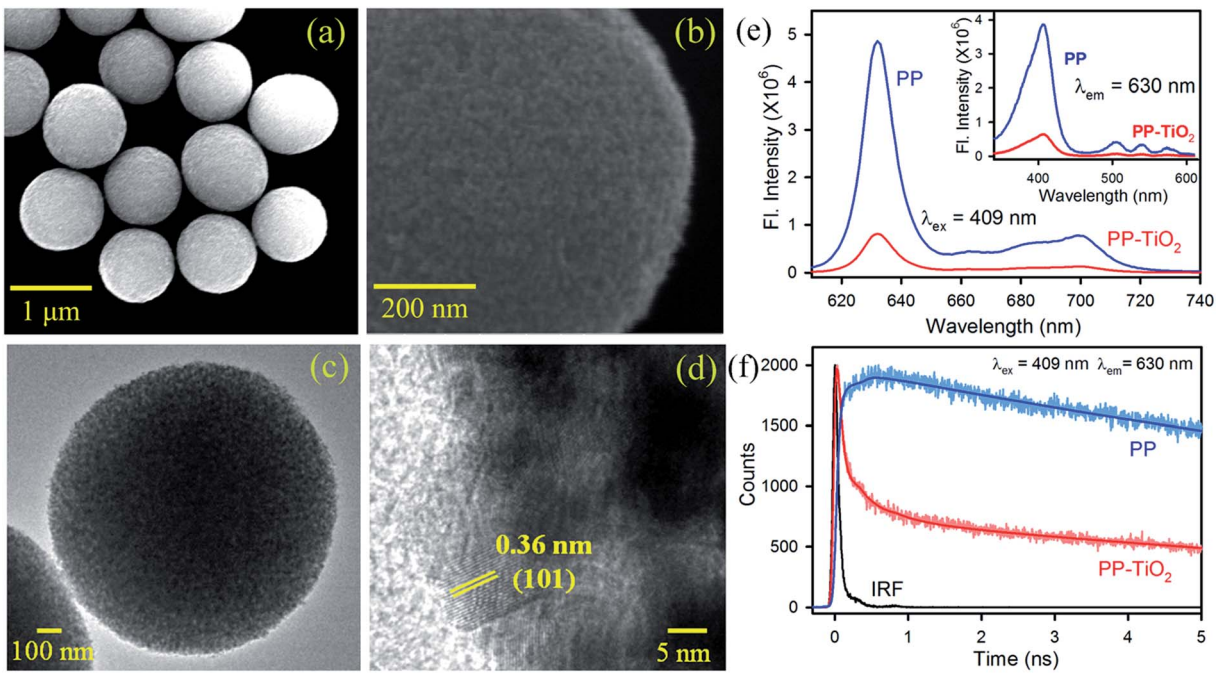

Fig. 1 (a and b) SEM and (c and d) TEM images of the TiO_2 MS. (e) Room-temperature PL spectra (excitation at 409 nm) of free PP (blue) and PP–TiO_2 MS (red). The inset shows the excitation spectra monitored at 630 nm. (f) Fluorescence decay profiles of PP (blue) and PP–TiO_2 MS (red) at 630 nm (with excitation at 409 nm).

for a further 12 h. To remove the unbound dye, the prepared nanohybrids were washed several times with DMSO/water (1 : 1). The nanohybrids were dried by heating in a water bath and were stored in the dark. The functionalized mesh was dipped into the 0.5 mM PP solution and kept for 12 hours under dark. After the sensitization process, the mesh was washed several times with DMSO, dried in a water bath, and then stored in the dark until further use.

2.5. Characterization methods

The surface morphology of the samples was investigated *via* field emission scanning electron microscopy (FESEM, QUANTA FEG 250). Transmission electron microscopy (TEM) was carried out using an FEI (Technai S-Twin) instrument with an acceleration voltage of 200 kV. A carbon-coated copper grid was used to prepare the sample and the particle sizes were determined from the images obtained at the high magnification of 100 000×. For steady-state optical measurements, the absorption and emission spectra were obtained using a Shimadzu UV-2600 spectrophotometer and a Jobin Yvon Fluoromax-3 fluorimeter, respectively. Picosecond resolution fluorescence studies were performed using a time-correlated single photon counting (TCSPC) apparatus obtained from Edinburgh Instruments (instrument response function, IRF = 80 ps, excitation at 375 nm). The details of the experimental setup and methodology have been described in our earlier report.[11]

2.6. Adsorption tests and recharging

For the adsorption test, 0.1 mg of the FMs was taken in 2 mL of water and BP dissolved in acetonitrile was added. The adsorption kinetics were monitored with time by obtaining the absorption spectra. For photorecharging, BP adsorbed on the FMs surface was irradiated with visible light for 24 h. For chemical recharging, BP adsorbed on FM was rinsed with acetonitrile where BP dissolved in acetonitrile and the FM surface was cleaned.

3. Results and discussion

3.1. Structural and optical characterization of the functional microspheres (FMs)

TiO_2 MS were synthesized using a literature procedure[10b] and their detailed characterization has been documented in our earlier studies.[10c,10d] Scanning electron microscopy (SEM) images of the synthesized TiO_2 MS with a diameter of ~1–1.1 μm are shown in Fig. 1a. The high-resolution SEM image, as shown in Fig. 1b, clearly reveals the presence of densely packed TiO_2 nanocrystals. The high-resolution transmission electron microscopy (HRTEM) images of the MS are shown in Fig. 1c and d. The higher porosity and the composition of the MS with nanoparticle sizes of 10–20 nm can be clearly observed. To confirm the formation of functional microspheres (FMs) comprising TiO_2 MS sensitized with the biologically important dye protoporphyrin IX (PP), steady state and time-resolved fluorescence studies were performed. The strong fluorescence intensities of PP in the range of 620–720 nm were significantly quenched in the presence of TiO_2 MS upon photoexcitation at 409 nm, which confirms the strong electronic interactions between PP and MS in the FMs (Fig. 1e). The inset of Fig. 1e shows the quenching of the fluorescence intensity in the excitation spectra of PP upon attachment to the TiO_2 MS when monitored at the emission peak (630 nm). The fluorescence transients of PP in the presence and absence of TiO_2 MS were measured upon excitation with a 409 nm laser and monitored at a wavelength of 630 nm. The spectroscopic and fitting parameters are shown in Table 1. The longer lifetime of PP quenches in the presence of MS. The observed decrease in the lifetime can be correlated with the electron transfer process from PP to TiO_2

Table 1 Dynamics of the picosecond-resolved luminescence transients of PP and FM[a]

Sample	τ_1 (ns)	τ_2 (ns)	τ_3 (ns)	τ_{avg} (ns)
PP (bare)			15.85 (100%)	15.85
PP–TiO_2 MS	0.03 (80.53%)	0.38 (8.05%)	11.43 (11.42%)	1.36

[a] The emission (monitored at 630 nm) was detected using laser excitation at 409 nm. The numbers in the parenthesis indicate the relative weights.

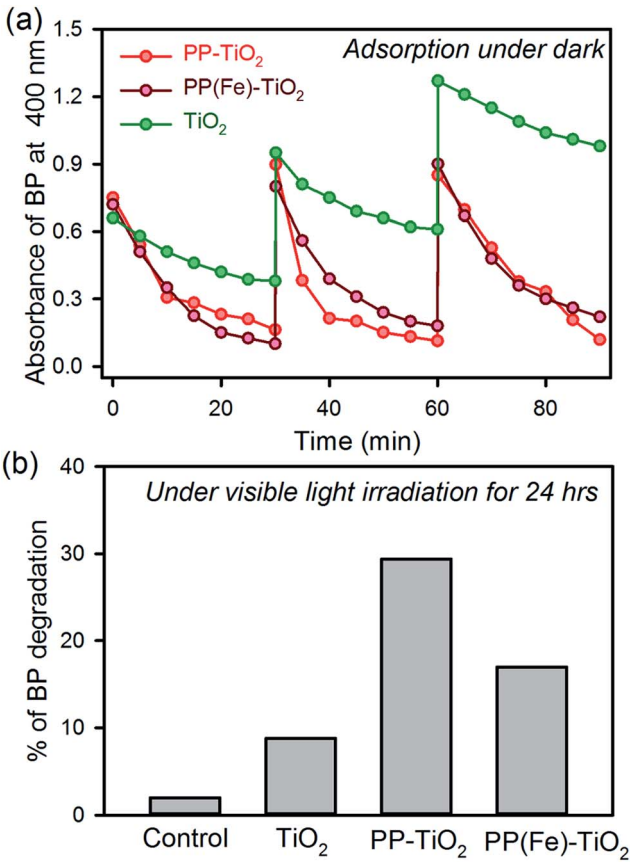

Fig. 2 (a) The adsorption kinetics of BP dispersed in water in the presence of TiO_2 MS, PP–TiO_2 MS, and PP(Fe)–TiO_2 MS under dark conditions. (b) The degradation of BP adsorbed on the surface of different materials under visible light irradiation for 24 h.

MS, which is consistent with that reported in the literature.[12] The time-resolved measurements confirm the formation of the nanohybrid (FMs).

3.2. Performance of the FM in the removal and degradation of BP

Fig. 2a shows the adsorption kinetics of BP dispersed in water on the surface of the FMs and other materials. The functionalized MS with PP shows faster adsorption kinetics than that of the MS only. The TiO_2 MS sample shows BP adsorption due to the porosity in the microspheres. In the presence of PP, the adsorption of BP significantly increases due to complex formation between BP and PP on the surface of the MS.[10d] The recyclability of the FMs was performed for three cycles and the activity was found to be intact, whereas the adsorption of BP decreased in each cycle in the case of MS only. The adsorption kinetics of the FMs in the presence of iron ions in the PP cavity (PP(Fe)–TiO_2) were also performed, as shown in Fig. 2a, as PP in hemoglobin contains iron in its central cavity and the ion is omnipresent in the aqueous environment. The adsorption kinetics and recyclability were found to be unaltered in the presence of iron. Thus, the metallated PP present in the hemoglobin can be directly used to synthesize the FMs. To recharge the FM, two methods were employed. One was the photodegradation of BP under visible light irradiation in the presence of FM.[13] The highest degradation was observed in the presence of FM, whereas the presence of iron decreased the photodegradation of BP due to the trapping of photoexcited electrons by iron ions, as previously reported.[11a] The other recharging technique was the dissolution of BP in acetonitrile. In all the cases, dissolution of BP adsorbed on the FM and that of other materials in acetonitrile was found to be 100%. Thus, the FM can be recharged using any of the two abovementioned methods.

3.3. Fabrication and performance of the prototype device

After the confirmation of the efficient removal of BP dispersion in water using the FMs, a prototype flow device was constructed, as shown in Fig. 3c. To fabricate the flow device, a stainless steel mesh was functionalized with the FMs (activated mesh). SEM images of the activated mesh are shown in Fig. 3a and b. The activated mesh was placed in a syringe in a way that the BP dispersion in water flew through the mesh (Fig. 3c). The BP removal activity and recyclability of the activated filter were checked for three sets, as shown in Fig. 3d–f. Five cycles were performed in each set with 2 mL of a 0.2×10^{-3} M BP

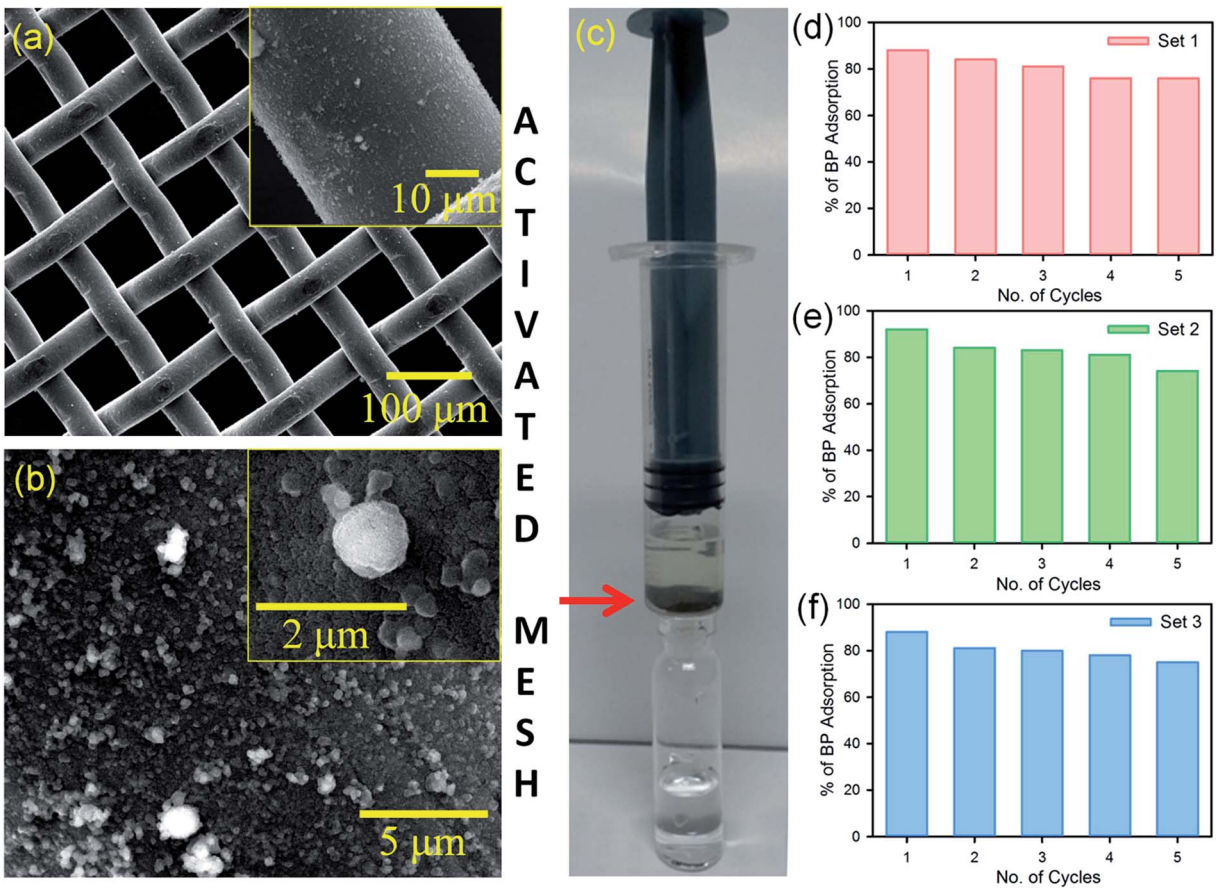

Fig. 3 (a and b) SEM images of the PP-sensitized TiO_2 MS on stainless steel mesh (activated mesh). (c) The prototype flow device fabricated using the activated mesh. (d–f) BP removal using the flow device in different sets. Chemical recharging of the activated mesh using acetonitrile was performed after each set.

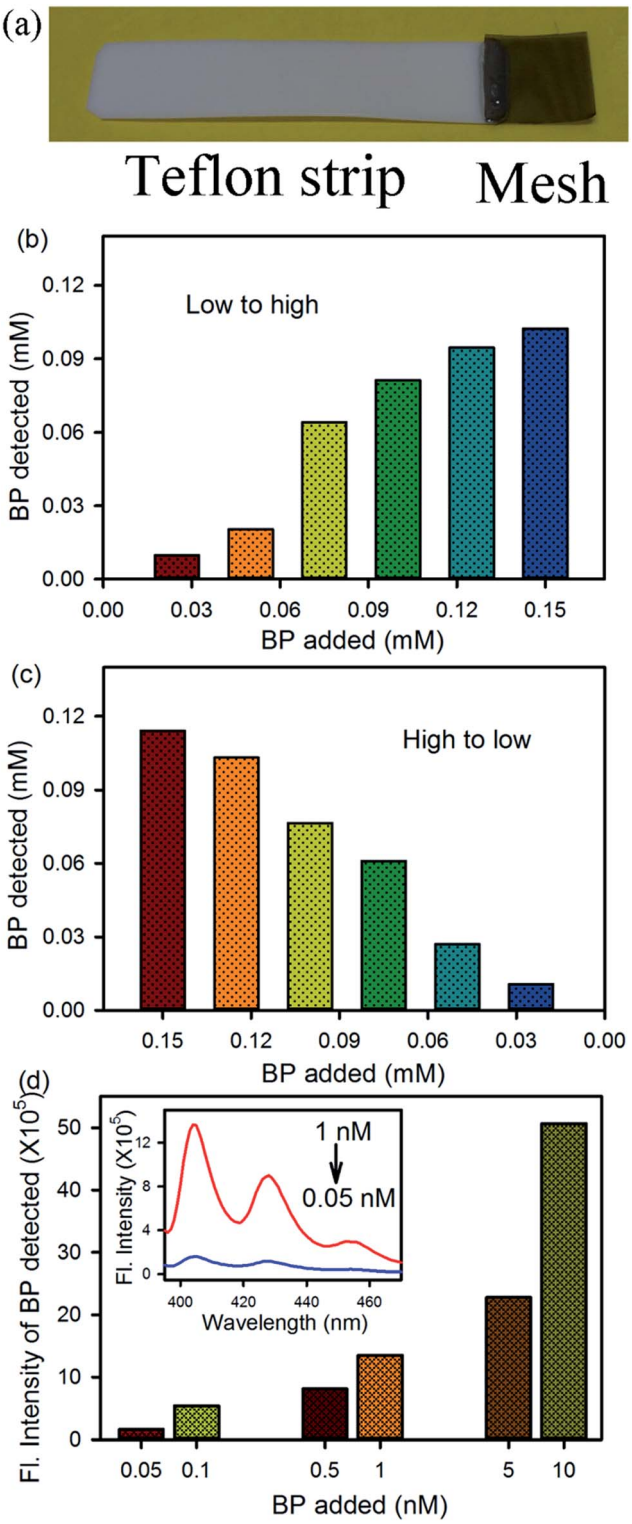

Fig. 4 (a) An assessment strip made up of a Teflon strip and the activated mesh. (b and c) The detection of BP from a water dispersion at various concentrations from low to high and high to low, respectively, using absorption spectroscopy. (d) The detection of BP from a water dispersion at various concentrations using a fluorometric assay. The inset shows the emission spectra of BP in acetonitrile upon excitation at 350 nm.

dispersion in water in each cycle. After each set, the mesh was recharged (cleaned) by rinsing the mesh in acetonitrile for 5 min. After three sets, the device was found to adsorb BP with ~80% efficiency. The experimental results shown in the Fig. 3 suggest the excellent adsorption and recyclability of the prototype device using the activated mesh.

3.4. Assessment strip for the detection of BP

An assessment strip was also designed, as shown in Fig. 4a, using the activated mesh for the rapid onboard monitoring of BP contamination in any aqueous environment. The activated mesh (1 cm^2 area) was fixed with a Teflon strip using glue. The strip was dipped into a BP dispersion in water for 5 min under constant stirring, and then the strip was rinsed with 2 mL of acetonitrile solvent, where the BP was solubilized in acetonitrile and the FMs remained attached to the mesh. The concentration of BP was detected using absorption and fluorescence spectra of the acetonitrile solution containing BP only. Fig. 4b and c shows the detection of the BP dispersion present in water at various concentrations from low to high and high to low, respectively. In both the cases, BP was detected in the ppm level using absorption spectroscopy. To detect the very low concentration of BP in an aqueous environment, a fluorometric assay was performed. In the present case, the emission spectra of the acetonitrile solution containing BP was obtained upon excitation at 350 nm and the emission intensity at 405 nm was plotted, as shown in Fig. 4d. The inset shows the full emission spectra at two different concentrations of BP. Using the fluorometric assay, a ppt level of BP present in the water can be detected. Thus, the two types of prototype devices may be used for the detection and removal of BP contamination in any aqueous environment.

4. Conclusion

In summary, TiO_2 microspheres were synthesized *via* a facile solvothermal method and were duly sensitized with protoporphyrin IX dye for potential use as functional microspheres (FMs) for the remediation of benzo[*a*]pyrene exposure in aqueous environments. The FMs were found to remove BP from aquatic environments with cent percent efficiency in a very short time. The effect of the presence of the dye and the incorporation of iron ion in the central cavity of the dye was investigated. While the central iron ion was found to have no effect on BP removal, the PP sensitization was extremely important for the activity of the FMs. Complexation of BP with PP on the FMs surface was concluded to be the reason for the efficient activity of the FMs. We showed that the recharging of the FMs for reinstating their function can be carried out using two methods. First, through solar irradiation, where the adsorbed BPs are photodegraded with limited efficiency. In the second case, the adsorbed BPs can be recovered using a non-aqueous solvent, such as acetonitrile, with cent percent efficiency. We demonstrated that the FMs can be attached on a stainless steel mesh for real-world aquatic applications including emergency cleaning in an accidental oil spillage in

a marine environment. Moreover, we showed that the FM-containing mesh can be used for the assessment of BP in any aquatic environment with ppt sensitivity using an associated fluorometric assay. Overall, the developed materials and strategy will be extremely useful for wastewater management.

Author contributions

Z. S. S., S. A. A., S. S., N. H. Y., M. A. and S. K. P. contributed equally in the design & performing experiments, data analysis and manuscript writing.

Acknowledgements

The authors wish to acknowledge the support of King Abdul Aziz City for Science and Technology (KACST) through the Science & Technology Unit (STU) at Umm Al-Qura University for funding through Project No. 12-NANO2317-10 as part of the National Science, Technology and Innovation Plan.

References

1 (*a*) R. Camilli, C. M. Reddy, D. R. Yoerger, B. A. S. Van Mooy, M. V. Jakuba, J. C. Kinsey, C. P. McIntyre, S. P. Sylva and J. V. Maloney, *Science*, 2010, **330**, 201–204; (*b*) F. Yin, J. S. Hayworth and T. P. Clement, *PLoS One*, 2015, **10**, e0118098.

2 (*a*) S. B. Joye, *Science*, 2015, **349**, 592–593; (*b*) C. H. Arnaud, *Chem. Eng. News*, 2015, **93**, 7.

3 (*a*) B. Gonzalez-Gaya, M.-C. Fernandez-Pinos, L. Morales, L. Mejanelle, E. Abad, B. Pina, C. M. Duarte, B. Jimenez and J. Dachs, *Nat. Geosci.*, 2016, **9**, 438–442; (*b*) C. Le Quéré, R. Moriarty, R. M. Andrew, J. G. Canadell, S. Sitch, J. I. Korsbakken, P. Friedlingstein, G. P. Peters, R. J. Andres, T. A. Boden, R. A. Houghton, J. I. House, R. F. Keeling, P. Tans, A. Arneth, D. C. E. Bakker, L. Barbero, L. Bopp, J. Chang, F. Chevallier, L. P. Chini, P. Ciais, M. Fader, R. A. Feely, T. Gkritzalis, I. Harris, J. Hauck, T. Ilyina, A. K. Jain, E. Kato, V. Kitidis, K. Klein Goldewijk, C. Koven, P. Landschützer, S. K. Lauvset, N. Lefèvre, A. Lenton, I. D. Lima, N. Metzl, F. Millero, D. R. Munro, A. Murata, J. E. M. S. Nabel, S. Nakaoka, Y. Nojiri, K. O'Brien, A. Olsen, T. Ono, F. F. Pérez, B. Pfeil, D. Pierrot, B. Poulter, G. Rehder, C. Rödenbeck, S. Saito, U. Schuster, J. Schwinger, R. Séférian, T. Steinhoff, B. D. Stocker, A. J. Sutton, T. Takahashi, B. Tilbrook, I. T. van der Laan-Luijkx, G. R. van der Werf, S. van Heuven, D. Vandemark, N. Viovy, A. Wiltshire, S. Zaehle and N. Zeng, *Earth Syst. Sci. Data*, 2015, **7**, 349–396.

4 (*a*) C. M. Reddy, J. S. Arey, J. S. Seewald, S. P. Sylva, K. L. Lemkau, R. K. Nelson, C. A. Carmichael, C. P. McIntyre, J. Fenwick, G. T. Ventura, B. A. S. Van Mooy and R. Camilli, *Proc. Natl. Acad. Sci. U. S. A.*, 2012, **109**, 20229–20234; (*b*) J. Gros, D. Nabi, B. Würz, L. Y. Wick, C. P. D. Brussaard, J. Huisman, J. R. van der Meer, C. M. Reddy and J. S. Arey, *Environ. Sci. Technol.*, 2014, **48**, 9400–9411.

5 C. P. D. Brussaard, L. Peperzak, S. Beggah, L. Y. Wick, B. Wuerz, J. Weber, J. Samuel Arey, B. van der Burg, A. Jonas, J. Huisman and J. R. van der Meer, *Nat. Commun.*, 2016, **7**, 11206.

6 K. Ziervogel, L. McKay, B. Rhodes, C. L. Osburn, J. Dickson-Brown, C. Arnosti and A. Teske, *PLoS One*, 2012, **7**, e34816.

7 A. Steen and A. Findlay, *International Oil Spill Conference Proceedings*, 2008, **2008**, 645–649.

8 S. Kleindienst, J. H. Paul and S. B. Joye, *Nat. Rev. Microbiol.*, 2015, **13**, 388–396.

9 L. Luo, X. Lai, B. Chen, L. Lin, L. Fang, N. F. Y. Tam and T. Luan, *Sci. Rep.*, 2015, **5**, 12776.

10 (*a*) B. Liu, L.-M. Liu, X.-F. Lang, H.-Y. Wang, X. W. Lou and E. S. Aydil, *Energy Environ. Sci.*, 2014, **7**, 2592–2597; (*b*) Z.-Q. Li, Y.-P. Que, L.-E. Mo, W.-C. Chen, Y. Ding, Y.-M. Ma, L. Jiang, L.-H. Hu and S.-Y. Dai, *ACS Appl. Mater. Interfaces*, 2015, **7**, 10928–10934; (*c*) Z. S. Seddigi, S. A. Ahmed, S. Sardar and S. K. Pal, *Sci. Rep.*, 2016, **6**, 23209; (*d*) Z. S. Seddigi, S. A. Ahmed, S. Sardar and S. K. Pal, *Photochem. Photobiol. Sci.*, 2016, **15**, 920–927.

11 (*a*) S. Sardar, S. Sarkar, M. T. Z. Myint, S. Al-Harthi, J. Dutta and S. K. Pal, *Phys. Chem. Chem. Phys.*, 2013, **15**, 18562–18570; (*b*) S. Sardar, P. Kar and S. K. Pal, *Journal of Materials NanoScience*, 2014, **1**, 12–30; (*c*) S. Sardar, P. Kar, H. Remita, B. Liu, P. Lemmens, S. K. Pal and S. Ghosh, *Sci. Rep.*, 2015, **5**, 17313.

12 S. Sardar, S. Chaudhuri, P. Kar, S. Sarkar, P. Lemmens and S. K. Pal, *Phys. Chem. Chem. Phys.*, 2015, **17**, 166–177.

13 F. Venditti, F. Cuomo, A. Ceglie, P. Avino, M. V. Russo and F. Lopez, *Langmuir*, 2015, **31**, 3627–3634.

